Theoret. Appl. Mech., Vol.32, No.4, pp. 359–384, Belgrade 2005

Stability of narrow-gap MHD Taylor-Couette flow with radial heating and constant heat flux at the outer cylinder

R.K. Deka *

Abstract

A linear stability analysis has been presented for hydromagnetic dissipative Couette flow, a viscous electrically conducting fluid between rotating concentric cylinders in the presence of a uniform axial magnetic field and constant heat flux at the outer cylinder. The narrow-gap equations with respect to axisymmetric disturbances are derived and solved by a direct numerical procedure. Both types of boundary conditions, conducting and non-conducting walls are considered. A parametric study covering on the basis of μ, the ratio of the angular velocity of the outer cylinder to that of inner cylinder, Q, the Hartmann number which represents the strength of the axial magnetic field, and N, the ratio of the Rayleigh number and Taylor number representing the supply of heat to the outer cylinder at constant rate is presented. The three cases of $\mu < 0$ (counter rotating), $\mu > 0$ (co-rotating) and $\mu = 0$ (stationary outer cylinder) are considered wherein the magnetic Prandtl number is assumed to be small. Results show that the stability characteristics depend mainly on the conductivity on the cylinders and not on the heat supplied to the outer cylinder. As a departure from earlier results corresponding to isothermal as well as hydromagnetic flow, it is found that the critical wave number is strictly a monotonic

*Department of Mathematics, Gauhati University, Guwahati-781 014, India

decreasing function of Q for conducting walls. Also, the presence of constant heat flux leads to a fall in the critical wave number for counter rotating cylinders, which states that for large values of -μ, there occur transition from axisymmetric to non-axisymmetric disturbance whether the flow is hydrodynamic or hydromagnetic and this transition from axisymmetric to non-axisymmetric disturbance occur earlier as the strength of the magnetic field increases.

Keywords: hydrodynamic and hydromagnetic flow, non-axisymmetric disturbance, critical wave number, rotating concentric cylinders, linear stability analysis

1 Introduction

Taylor-Couette flow is one of the most important examples of fluid systems that exhibit the spontaneous formation of increasingly complex dynamic flow structures. The Couette apparatus was developed by Couette [1] as a means for measuring the viscosity of a fluid at small-imposed angular velocities of the cylinders. This occurs through a sequence of transitions, which takes place as the drive is increased. At small angular velocities of the inner cylinder (Ω_1) the flow driven around, it is purely azimuthal (circular Couette flow, or CCF). Taylor [2] found that when the angular velocity of the inner cylinder exceeds some critical value, then the circular Couette flow becomes unstable to axisymmetric perturbations. The radial and axial velocity components grow exponentially in time and then saturate nonlinearly to a flow pattern, which consists of axisymmetric vortices stacked on top of one another in the axial direction, with radial inflows and outflows. This is what we now know as Taylor vortex flow (TVF). If the rotation rate of the inner cylinder is further increased TVF becomes unstable to non-axisymmetric perturbations, and azimuthal waves are formed which rotate around the inner cylinder at some wave speed (wavy modes). A further increase in the rotation rate of the inner cylinder leads to an even wider variety of flows, each with clearly defined stability boundaries, due to the exact way in which more and more spatial and temporal symmetries are broken, Taylor-Couette flow is an ideal setting in which to study instabilities and nonlinear behavior in a fluid system.

This article is concerned with that of hydromagnetic Couette flow; in this case the fluid contained within the narrow-gap of coaxial cylinders is electrically conducting (such as liquid sodium, gallium or mercury) and an external magnetic field is applied keeping the cylinders at different temperatures with constant heat flux at the outer cylinder. This problem is also interesting because of its important applications for the gaseous core nuclear reactors and power-generating devices. Using the infinite cylinders approximation, Chandrasekhar [3] calculated the linear stability of both hydrodynamic and hydromagnetic Couette flow, not only for the simple case of the inner cylinder rotating, but also for co- and counter rotating cylinders. Experimentally, Donnelly & Ozima [4] and Donnelly & Caldwell [5] confirmed the results of Chandrasekhar using mercury contained between Perspex and stainless steel cylinders, although not much differences were found between the different boundary conditions (insulating and conducting) in the two cases. The boundary conditions in the hydromagnetic case are not trivial, and were described with clarity by Roberts [6], who also performed calculations on the stability of non-axisymmetric perturbations. Tabelling [7], using a method similar to Davey's [8] amplitude expansion, calculated the effective viscosity of axisymmetric flow in the TVF regime and compared with Donnelly's [4] experiments which indicate that the onset of wavy vortices is significantly inhibited by the magnetic field. Nagata [9] has more recently investigated nonlinear solutions in the planar geometry, and Hollerbach [10] shows Taylor's cells in spherical geometry. Willis & Barenghi [11] developed a numerical formulation based on spectral methods suitable to study three-dimensional nonlinear hydrodynamic Taylor-Couette flow and compared with experiment. When only the inner cylinder is rotated it was found that the critical value for the onset of non-axisymmetric motion was just above the critical value in the hydrodynamic case. Takhar et al. [12] further showed the amplitude of the radial velocity and the cell-pattern on graphs for axisymmetric disturbances and for both conducting and non-conducting walls with several different values of μ and Q. Chen & Chang [13] studies the hydromagnetic Couette flow for small-gap equations with respect to non-axisymmetric disturbances and presented an analysis for the stationary as well as oscillatory critical mode. Recently, Willis & Barenghi [14] investigated magnetic Taylor-Couette flow in the non-linear regime. In the presence of an axial magnetic field the Lorentz force was found to have a

significant damping effect at larger length scales as a consequence of the small magnetic Parndtl number limit. The significant enhanced stability was observed at only small-imposed field strengths.

The linear stability analysis of CCF in a weak magnetic field at various radius ratios has been studied by Soundalgekar et al. [15] and the combined effect of radial temperature gradient and constant heat flux at the outer cylinder has been studied by Ali et al. [16] for hydrodynamic case with narrow gap geometry, which motivates to undertake the present study for the effect of radial temperature gradient and constant heat flux at the outer cylinder for hydromagnetic case. The plan of this article is the following. In §2 we present the governing MHD equations coupled with the energy equation and the boundary conditions, and introduce the small Prandtl number limit, which is relevant to liquid metals available in the laboratory. In §3, we present results and discussion in the small Prandtl number limit with the consideration of the effect of constant heat flux at the outer cylinder and in §4 the summary is spelt out. A systematic study which covers $-1.0 \leqslant \mu \leqslant 1.0$ is presented for low as well as high values of the Hartmann number Q for N ¿ 0. Here N, being the parameter characterizing the supply of heat flux at the outer cylinder. Results for three typical cases are reported. These belong to the flow between (i) a rotating inner wall with a stationary outer wall, (ii) counter-rotating walls, and (iii) co-rotating walls.

2 Problem formulation and method of solution

Let r, θ and z denote the usual cylindrical polar coordinates, and let u_r, u_θ, u_z and H_r, H_θ and H_z denote the components of velocity and magnetic field intensity, respectively. We consider two infinitely long concentric circular cylinders with the z-axis as their common axis and let the radii and angular velocities of the inner and outer cylinders are R_1, R_2 and Ω_1, Ω_2, respectively. The equations of motion and energy equation for an incompressible, viscous electrical conducting fluid in the presence of a uniform magnetic field in the axial direction and constant heat flux at the outer cylinder admit of a steady solution,

$$\left.\begin{aligned} &u_r = u_z = 0, u_\theta = V(r) = Ar + B/r, \overline{T} = T_1 + \frac{qR_2}{K}\ln\frac{r}{R_1} \\ &H_r = H_\theta = 0, H_z = H = \text{constant} \end{aligned}\right\} \quad (1)$$

where

$$A = \frac{\mu - \eta^2}{1-\eta^2}\Omega_1, \quad \mathrm{B} = \frac{R_1^2(1-\mu)}{1-\eta^2}\Omega_1, \quad \eta = \frac{R_1}{R_2} \quad (2)$$

Clearly the solutions given in (1) are consistent with the following boundary conditions for velocity and temperature

$$\begin{aligned} &u_r = 0, \mathrm{u}_\theta = V(r) = \Omega_1 R_1, \mathrm{u}_\mathrm{z} = 0, \overline{T} = T_1 \quad at \quad r = R_1 \\ &u_r = 0, \mathrm{u}_\theta = V(r) = \Omega_2 R_2, \mathrm{u}_\mathrm{z} = 0, \frac{d\overline{T}}{dr} = \frac{q}{K} \quad at \quad r = R_2 \end{aligned} \quad (3)$$

In deriving the temperature distribution in (1) from the energy equation, viscous dissipation and energy associated with change in pressure are neglected. Here q is the uniform surface heat flux; K the thermal conductivity of the fluid and T_1 is the temperature of the inner cylinder.

To study the stability of this flow we superimpose a general disturbance on the basic solution, substitute it in the governing equations and neglect quadratic terms in the usual way. Since the coefficients in the resultant disturbance equations depend only on r, it is possible to look for solutions of the form

$$u_\theta = \{V(r) + \mathrm{v}(r)\}e^{\sigma t}\cos\lambda z \quad (4)$$

where $v(r)$ is the azimuthal component of the small disturbance velocity, and with similar expressions for the other components of velocity, pressure, temperature and the components of magnetic field intensity. It is assumed that the axial wave length λ be real. The parameter σ is the complex

growth rate. In view of the physical similarity of this problem with Taylor's stability problem of Couette flow; it is likely that in the present problem also the onset of stability will be as a steady secondary flow. Thus when the marginal state is stationary we may put $\sigma = 0$ in (4). In the present analysis we will be concerned with the narrow-gap case in which the gap d $= R_2 - R_1$ is small compared to R_1 so that terms of $O(d/R_1)$ can be neglected. The derivation of the narrow-gap equations in our study are the same as those derived by Takhar et al.[17] except that now we must consider the constant heat flux at the outer cylinder. The scaling for u and θ are $\nu/2Ad^2$, $\mu C_p q/(2AK^2)$ used to non-dimensionalize. We introduce further the following non-dimensional variables for radial variable and wave length as:

$$x = \frac{r - R_1}{d}, a = \lambda d \tag{5}$$

Now we define the Taylor number, Prandtl number, magnetic Prandtl number, and Hartmann number Q as:

$$T = -\frac{4A\Omega_1 d^4}{\nu^2}, \mathrm{Pr} = \frac{\mu \mathrm{C_p}}{\mathrm{K}}, P_m = \frac{\nu}{e}, Q = \frac{\mu_e H^2 d^2}{4\pi\rho\nu e} \tag{6}$$

where μ_e, e, C_p, ρ, ν are the magnetic permeability, electric resistivity, specific heat of the fluid, density and kinematic viscosity, respectively. Here, α appears from the Boussinesque approximation as the coefficient of cubical expansion. After combining the governing equations of perturbations, we obtain the following system of ordinary differential equations:

$$[(D^2 - a^2)^2 + Qa^2]u = -a^2 TG(x)[(D^2 - a^2)g + NG(x)\theta] \tag{7}$$

$$[(D^2 - a^2)^2 + Qa^2]g = u \tag{8}$$

$$(D^2 - a^2)\theta = u \tag{9}$$

where $D = d/dx, G(x) = 1 - (1 - \mu)x$, and g represents the azimuthal component of the small disturbance magnetic field.

Here, N is the ratio of a Rayleigh number,

$$Ra = \frac{\alpha d^4 \,\mathrm{Pr}}{\nu^2}\beta R_{LM}\Omega_1^2$$

and the Taylor number based on the centrifugal acceleration $R_{LM}\Omega_1^2$ with $R_{LM} = R_1/\eta$ and $\beta = q/K$ being the adverse temperature gradient which is maintained

It is known that the onset of Taylor vortices in the hydromagnetic case depends strongly on the conductivity of the containers and also on the magnetic Prandtl number. It has been found that if the magnetic Prandtl number is of order 1, then the presence of the magnetic field is strongly destabilizing and the Hartmann number Q does not have to be very large for there to be an effect. For example, $Q \sim O$ (10) is enough to cause significant destabilization. For the sake of comparison it is worth noting that $Q \sim O(10^3)$ was achieved in the experiments of Donnelly & Ozima [4]. However, if the magnetic Prandtl number is reduced and approaches realistic values for laboratory liquid metals, this destabilization disappears, and the application of a magnetic field is strongly stabilizing. Following these terrestrial conditions, we let the magnetic Prandtl number to be small, since laboratory liquid metals generally have very small Prandtl numbers, for example, for liquid sodium $P_m \sim O(10^{-5})$ and for mercury $P_m \sim O(10^{-7})$.

The derivation of the boundary conditions for the magnetic field is somewhat more involved, due to the fact that they depend on the conductivity of the cylinders. For the sake of mathematical convenience it is often assumed in the literature that the cylinders are either perfectly insulating (so the conductivity is exactly zero) or perfectly conducting (so the conductivity tends to infinity). We refer the reader to Willis & Barenghi [18] and Roberts [6] who determined boundary conditions for cylinders of arbitrary conductivity, and do not repeat here again. Accordingly, the appropriate boundary conditions at x = 0 and x = 1 for non-conducting walls are

$$\left.\begin{aligned} u = Du = g = (D^2 - a^2)g = \theta = 0 \quad \text{at} \quad \mathrm{x} = 0 \\ u = Du = g = (D^2 - a^2)g = D\theta = 0 \quad \text{at} \quad \mathrm{x} = 1 \end{aligned}\right\} \qquad (10)$$

and for conducting walls are

$$\left.\begin{aligned} u = Du = Dg = (D^2 - a^2)g = \theta = 0 \quad \text{at} \quad \text{x} = 0 \\ u = Du = Dg = (D^2 - a^2)g = D\theta = 0 \quad \text{at} \quad \text{x} = 1 \end{aligned}\right\} \tag{11}$$

The homogenous set of equations (7)-(9) with the boundary conditions (10) or (11) determine an eigenvalue problem of the form

$$F(\mu, Q, N, a, T) = 0 \tag{12}$$

For given values of μ, Q, N, which determine the basic state velocity, temperature and magnetic field strength, we seek the minimum real positive T for which there is a non-trivial solution for (12). The value of T sought is the critical Taylor number T_c for assigned values of μ, Q, and N. The value of a corresponding to T_c which determine the form of the critical disturbance is called critical wave number. We solve the two point eigenvalue problem defined by (7)-(9) using (10) or (11) by a shooting technique together with a unit disturbance method. Indeed, there are many analytical methods, which can be used in the stability analysis, for example, the work done by Weinstein [19, 20] for wavy vortices in the flow between two long concentric rotating cylinders. The method used in the present study has also been widely used by several workers for similar hydrodynamic stability problems, for example Chen & Chang [13], Chen & Chang [21] and Deka & Takhar [22]. For details, the reader is referred to Harris & Reid [23]. In order to obtain a faster convergence of the iteration, we use the modified algorithm developed by Chen & Chang [21] for this eigenvalue problem.

3 Results and discussion

Takhar et al. [17] studied the instability of hydromagnetic dissipative Couette flow with respect to axisymmetric disturbances in the presence of radial temperature gradient and axial magnetic field for narrow gap, which is a special case of present study with constant heat flux at the outer cylinder. So, we conduct calculations and check the results in terms of a_c and T_c

for both conducting and non-conducting walls with the corresponding data obtained by Takhar et al.[17] and presented in Table 1. The comparison is in good agreement.

We note that our stability analysis combines in one problem the simultaneous effects of radial temperature gradient due to a constant heat flux at the outer cylinder, axial magnetic field, and rotation velocities ratio. The study includes, as special cases, the stabilizing influence of only one or two factors, previously examined by different authors. Setting $Q = 0$ and $N = 0$, the governing equations reduce to those derived first by Taylor [2] under the narrow-gap approximations and then by Chandrasekhar [24]. When $Q = 0$ but $N \neq 0$, we recover the stability equations of radial temperature gradient obtained by Soundalgekar et al. [25]. Finally, when $N = 0$ but $Q \neq 0$, we come to the problem considered by Chandrasekhar [26] for an electrically conducting Couette flow with an axial magnetic field under narrow-gap assumptions.

We have calculated the critical values of a, T for various value of Q, N, and rotation ratio μ. In this study the range of N is taken from 0 to 1, rotation ratio from -1. to 1.0, Q from 10 to 300. The computed values with these parametric values are listed in Tables 1 - 7 for conducting as well as non-conducting walls. It is observed that owing to the supply of heat to the outer cylinder at constant rate, the critical value of the Taylor number decreases indicating less stable flow, for example, in the absence of axial magnetic field (Q = 0) the value of T_c for $N = 0$ is 18666 when $\mu = -1.0$ and the corresponding value of T_c for $N = 1.0$ is 9508. From these tables, further we observe that the critical Taylor number T_c decreases with N but increases with the strength of the magnetic field parameter Q. This indicates, the presence of a magnetic field for a viscous conducting fluid has a stabilizing effect. And for the same Q, the T_c for conducting walls is always higher than non-conducting walls, which means, the flow remains more stable between conducting walls. On the contrary, the imposition of constant heat flux at the outer cylinder is not inspiring for the stability of the flow.

The variation of T_c versus varying μ for assigned values of N are shown in figure 1 in the absence of axial magnetic field (Q = 0) and demonstrating the decreasing trend of critical Taylor number as the parameter N increases from 0 to 1, indicating unstable flow, where N = 0 corresponds to isothermal case. The corresponding variation of T_c versus N for both

conducting and non-conducting walls are presented in figures 2 and 3, for $\mu = -0.25, 0, 0.25$ and Q = 10 & 50 and it is observed that T_c is generally a monotonic decreasing function of N but increasing function of Q for all μ considered. This implies that the flow is no longer stable by the imposition of constant heat flux at the outer cylinder but stable due to the conductivity of the walls. The effect of radial temperature gradient together with the application of axial magnetic field to the electrically conducting fluid on the stability of Taylor-Couette flow has been studied by Takhar et al. [15] for narrow gap, predicting stabilizing effect due to negative temperature gradient. On the other hand, the effect of constant heat flux at the inner cylinder for narrow and wide gap has been studied by Takhar et al. [27, 28] and showed that constant heat flux at the inner cylinder too stabilizes the flow. Thus our result reflects that in the presence of constant heat flux at the outer cylinder, the stability of flow is delayed in comparison to the both isothermal and non-isothermal case as well as the application of constant heat flux at the inner cylinder. The variation of T_c versus μ are shown in figures 4 and 5, where the parameter μ is varied from -1.0 to 1.0 considering the moderate values of Q = 0, 50, 100 for both conducting as well as non-conducting walls. We observe from these figures that for counter rotating cylinders the flow is more stable in comparison to the co-rotating and stationary outer cylinder. Further, these figures show that the critical values of T_c increase as Q increases from 0 to a higher value. This means that the applied magnetic field always has a stabilizing effect on this flow. The variation of T_c with Q are presented in figures 6 and 7 for rotation ratios 0.5 and 1, since for $\mu = 0.5$ and 1, the disturbance is reported to be axisymmetric (Chen & Chang [19]). It is confirmed again that when $N \neq 0$, the critical values of Taylor number are lower than the values corresponding to N = 0 (isothermal case), for both conducting as well as non-conducting walls. Strikingly, we observe from figures 4 and 5 that, when $\mu < -0.9, N = 1, Q = 50$, the values of critical Taylor number attains a lower value. For hydrodynamic case, Krueger et al. [29] predicted for narrow-gap gap that when $\mu \leqslant -0.78$ the flow becomes non-axisymmetric when the cylinders are isothermal. There is growing evidence, both theoretical and experimental that when $\mu < -0.78$ (in the narrow gap approximation) instability sets in at a smaller value of the Taylor number with respect to non-axisymmetric disturbances (cf. Ref [30]). Thus, in agreement to their finding, in the presence of constant

heat flux at the outer cylinder, we have found that the stability sets at a smaller value of T_c for large $-\mu$. Also the fall in the values of T_c occurs earlier for large values of Q, viz; Q = 100 as shown in the graphs.

Now, we pay attention to the transition of the critical wave number a_c in the axial direction as Q and N increases for a given rotation ratio. In the presence of heat flux i.e. for N = 0, 0.25, 0.5, 0.75, 1.0 corresponding values of a_c for μ = -1.0 are 3.99, 3.80, 3.56, 3.27, 3.00 when the axial magnetic field is absent (Q = 0). This indicates that the critical axial wave length $2\pi d/a_c$ for which axisymmetric disturbances occur increases which implies that the spacing of the vortices remarkably increases. On the other hand, for conducting walls, Q = 10, 50, 100, 200, 300 the corresponding values of a_c are 4.16, 3.88, 3.50, 2.99, 2.66 when N = 1.0 for same $\mu = -1$, thereby showing the same decreasing trend of wavelength in the axial direction for conducting walls and it is true for non-conducting walls also and these are clearly demonstrated in figures 8 & 9 drawn for conducting and non-conducting walls for $-1 \leqslant \mu \leqslant 1$. The figures 8 and 9 are drawn when the parameter Q takes value of 0, 50, 100 for the two cases N = 0 (absence of constant heat flux) and N = 1. It has been observed from these two figures that the values of a_c corresponding to isothermal case, decreases with rotation ratio but increases monotonically for conducting walls and decreases for non-conducting walls in agreement with Chen & Chang [13], but in the presence of constant heat flux at the outer cylinder the trend reverses. For conducting fluid and isothermal case Chen & Chen [13] found a_c to be a monotonic decreasing function of Q when the walls are non-conducting, while for conducting walls, at first a_c increases monotonically with Q and then decreases. For N = 1, i.e. in the presence of constant heat flux at the outer cylinder, it is found that the critical values of wave number decreases monotonically as Q for both conducting as well as non-conducting walls. In other words, elongated Taylor cells will be observed for all Q in both the cases. However, when $\mu \leqslant -0.9$, the values of a_c takes a decreasing trend for Q = 0 in the presence of constant heat flux at the outer cylinder when N = 1. Thus the critical values of the wave number increase from a smaller value and reaches maximum near $\mu = -0.9$ and then decrease as μ decreases. This is due to the fact that for $\mu \leqslant -0.9$, the flow turns to become non-axisymmetric when $N \neq 0$. This transition occurs earlier as Q increases. In the cases for which non-axisymmetric disturbances occur, the critical value of a is less than the critical value of a

for an axisymmetric disturbance (see ref. [29]) and the critical wavelength $2\pi/\lambda = 2\pi d/a$, for non-axisymmetric disturbance will be slightly greater than the value for an axisymmetric disturbance at that value of μ. Thus, in conclusion, we can state that in the presence of constant heat flux and for large values of $-\mu$, the axisymmetric problem is irrelevant physically and one must consider the full three dimensional problem whether of the flow is hydrodynamic or hydromagnetic.

4 Conclusions

It is quite evident from our study that the vital contributions to the fluid stability comes from the magnetic field ($Q \neq 0$) rather than from applying constant heat flux at the outer cylinder as because the flow becomes strongly unstable when N $\neq 0$ and this is reflected for the cases of counter-rotating, co-rotating and stationary outer cylinder. The critical wave numbers are clearly a monotonic decreasing function of N as well as Q for both conducting as well as non-conducting walls. Also, in the presence of constant heat flux and for large values of $-\mu$, the axisymmetric problem is irrelevant physically and one must consider the full three-dimensional problem whether the flow is hydrodynamic or hydromagnetic and for $N \neq 0$, the transition from axisymmetric to non-axisymmetric disturbance occur earlier as the strength of the magnetic field increases.

Acknowledgement

This work was supported by University Grants Commission, New Delhi, India, vide letter No. F 30-1/2001 (SA-III) dt. 25.1.2002.

References

[1] Couette, M.F.A., *Annales de Chimie et de Physique*, **21**, 433 (1890).

[2] Taylor, G.I., *Proc. Roy. Soc. Lond. A.*, **223**, 289 (1923).

[3] Chandrasekhar, S., Hydrodynamic and Hydromagnetic Stability, Clarendon, 1961.

[4] Donnelly, R.J. and Ozima, M., *Proc. Roy. Soc. Lond. A*, **226**, 272 (1962).

[5] Donnelly, R.J. and Caldwell, D.R., *J. Fluid Mech.,* **19**, 257 (1963).

[6] Roberts, P.H., *Proc. Camb. Phil. Soc.,* **60**, 635 (1964).

[7] Tabelling, P., *J. Fluid Mech.*, **112**, 329 (1981).

[8] Davey, A., *J. Fluid Mech* **14**, 336 (1962).

[9] Nagata, M., *J. Fluid Mech.* **301**, 231 (1996)

[10] Hollerbach, R., *Physics of rotating fluids*, 295 (2000a)

[11] Willis, A.P. and Barenghi, C.F., 12^{th} International Couette-Taylor workshop, September 6-8, 2001, Evanston, IL, USA.

[12] Takhar, H.S., Ali, M.A. and Soundalgekar, V.M., *Appl. Sci. Res.,* **46**, 1 (1989).

[13] Chen, C.K. and Chang, M.H., *J. Fluid Mech.,* **366**, 135 (1998).

[14] Willis, A. P. and Barenghi, C.F., *J. Fluid Mech.*, **472**, 399 (2002).

[15] Soundalgekar, V.M., Ali, M.A. and Takhar, H.S., *Int. J. Energ. Res.* **18**, 689 (1994).

[16] Ali, M.A , Takhar, H.S. and Soundalgekar, V.M., *J. Appl. Mech.* **59**, 464 (1992).

[17] Takhar, H.S., Ali, M.A. and Soundalgekar, V.M., *Int. J. Energy Research* **16**, 597 (1992).

[18] Willis, A.P. and Barenghi, C.F., *J. Fluid Mech.,* **463**, 361 (2002).

[19] Weinstein, M., *Proc. Roy. Soc. Lond A*, **354**, 441 (1977a)

[20] Weinstein, M., *Proc. Roy. Soc. Lond A*, **354**, 441 (1977b).

[21] Chen, F. and Chang, M.H., *J. Fluid Mech.,* **243**, 243 (1992).

[22] Deka, R.K. and Takhar, H.S., *Int. J. Engng. Sci.* **42**, 953 (2004).

[23] Harris, D.L. and Reid, W.H., *J. Fluid Mech.* **20**, 95 (1964).

[24] Chandrasekhar, S., *Proc. Roy. Soc. Lond. A*, **246**, 301 (1958).

[25] Soundalgekar, V.M., Takhar, H.S. and Smith, T.J., *Wärme und Stoffübertragung* **15**, 233 (1981)

[26] Chandrasekhar, S., *Proc. Roy. Soc. Lond. A*, **216**, 293 (1953).

[27] Takhar, H.S., Ali, M.A. and Soundalgekar, V.M., *J. of the Franklin Institute*, **325(5)**, 609 (1988).

[28] Takhar, H.S., Ali, M.A. and Soundalgekar, V.M., *Wärme- und Stoffübertragung,* **22**, 23 (1988).

[29] Krueger, E.R., Gross, A. and DiPrima, R.C., *J. Fluid Mech.* **24**, 521 (1966).

[30] Drazin, P. G. and Reid, W.H., Hydrodynamic Stability, CUP (1981).

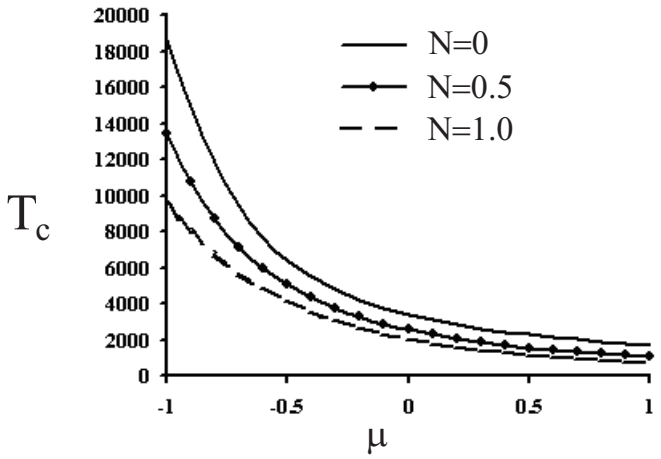

Figure 1: Variation of T_c with μ for assigned values of N (hydrodynamic case, Q = 0)

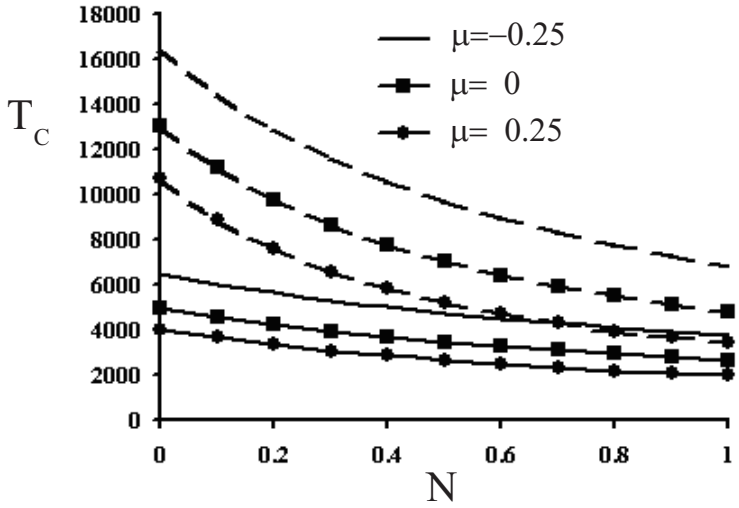

Figure 2: Variation of T_c with N for assigned values of μ and Q (Conducting walls). The solid curves are drawn for Q = 10, while the dashed are for Q = 50

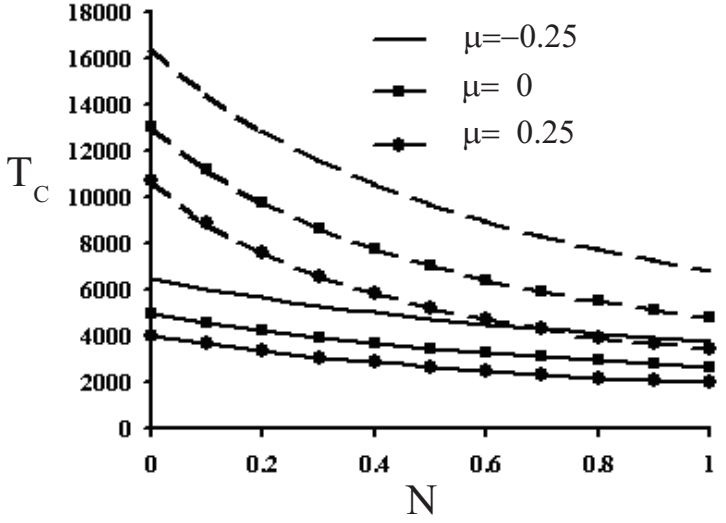

Figure 3: Variation of T_c with N for assigned values of μ and Q (non-Conducting walls). The solid curves are drawn for Q = 10, while the dashed are for Q = 50

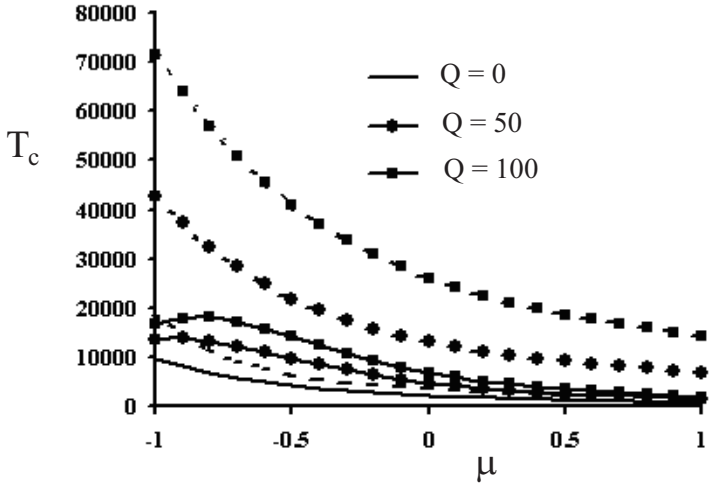

Figure 4: Variation of T_c with μ for assigned values of N and Q (Conducting walls). The solid curves are drawn for N = 1, while the dashed are for N = 0

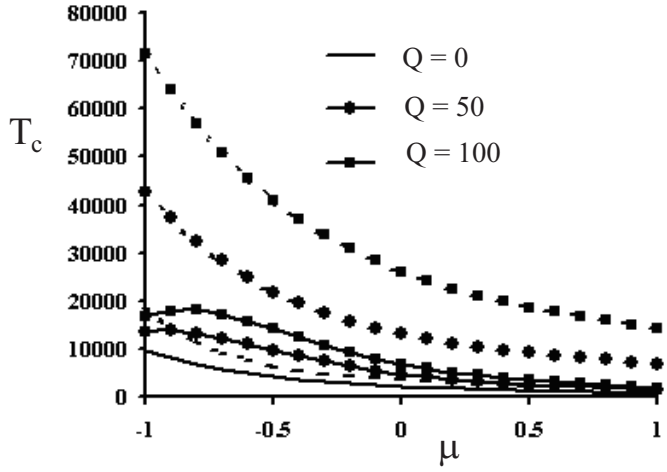

Figure 5: Variation of T_c with μ for assigned values of N and Q (non-Conducting walls). The solid curves are drawn for N = 1, while the dashed are for N = 0

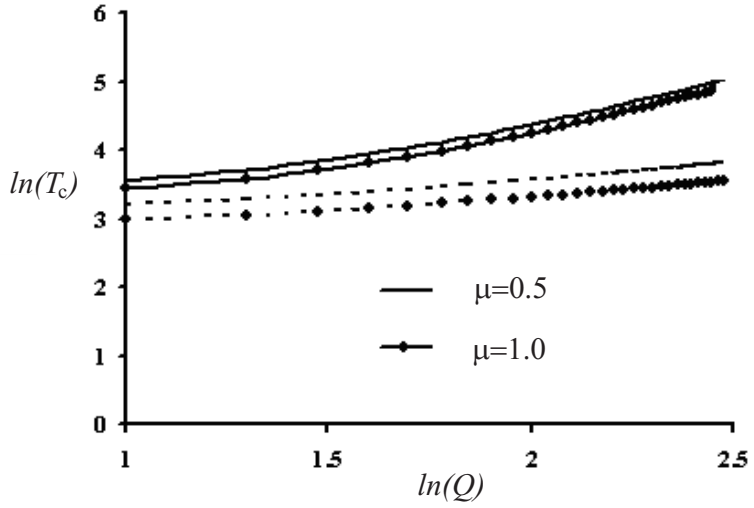

Figure 6: Variation of T_c with Q for assigned values of N. (Conducting walls). The solid curves are drawn for N = 0, while the dashed are for N = 1

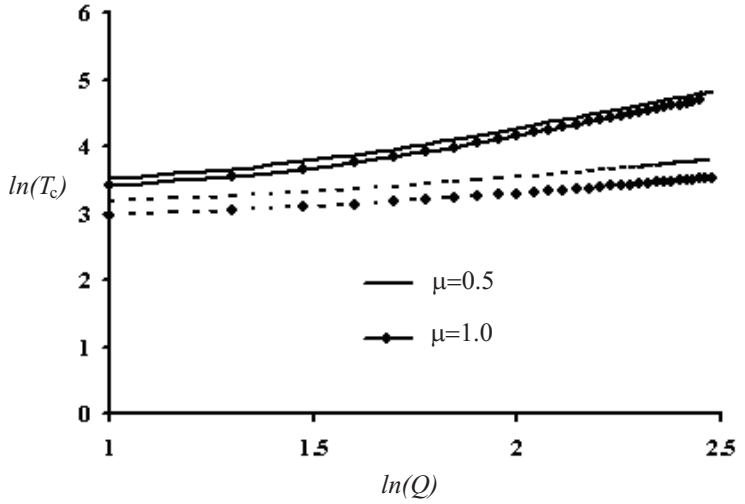

Figure 7: Variation of T_c with Q for assigned values of N. (non-Conducting walls). The solid curves are drawn for N = 0, while the dashed are for N = 1

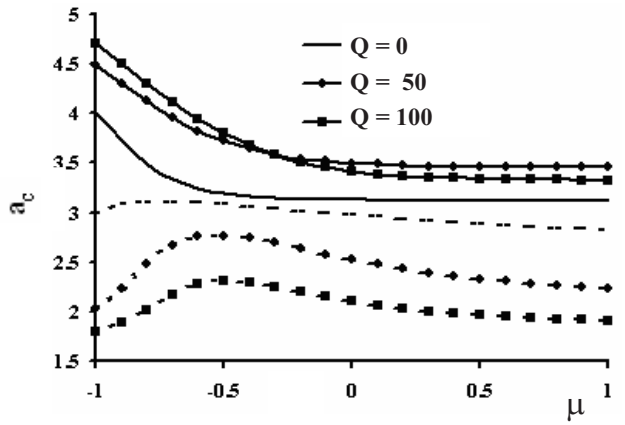

Figure 8: Variation of a_c with μ for assigned values of N and Q (Conducting walls). The solid curves are drawn for N = 0, while the dashed are for N = 1

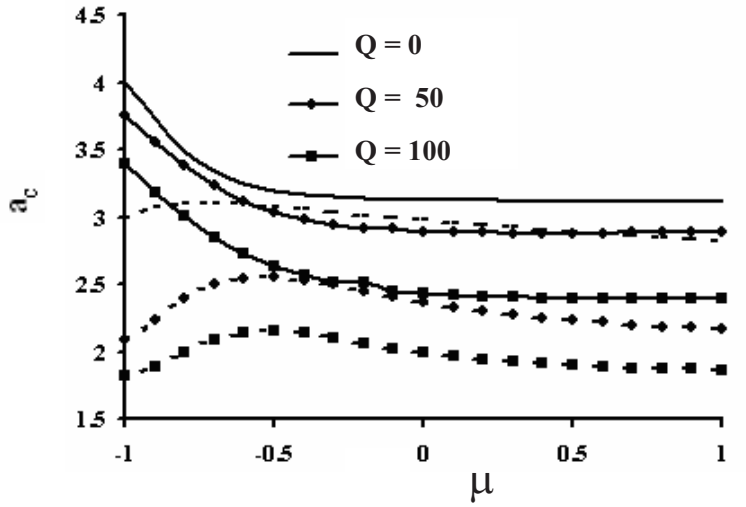

Figure 9: Variation of a_c with μ for assigned values of N and Q (non-Conducting walls). The solid curves are drawn for N = 0, while the dashed are for N = 1

		A		B	
μ	Q	a_c	T_c	a_c	T_c
-1	0	3.998	18666	3.999	18662
	10	4.167	24396	4.166	24390
	50	4.480	50796	4.481	50793
	100	4.698	91851	4.699	81849
-0.75	0	3.406	10518	3.406	10517
	10	3.661	15188	3.662	15186
	50	4.037	36758	4.038	36755
	100	4.209	70927	4.210	70919
	200	4.371	160858	4.370	168053
-0.5	0	3.197	6413	3.198	6413
	10	3.427	9809	3.427	9808
	50	3.720	26646	3.721	26643
	100	3.804	54581	3.801	54575
	200	3.769	129981	3.70	129975
	300	3.696	227581	3.700	227577
-0.25	0	3.144	4461	3.144	4461
	10	3.352	6954	3.352	6954
	50	3.563	19930	3.564	19929
	100	3.542	42422	3.544	42419
	200	3.307	104543	3.307	104542
	300	3.024	185057	3.024	185058
0	0	3.126	3389	3.127	3390
	10	3.326	5319	3.327	5319
	50	3.497	15576	3.498	15576
	100	3.417	33788	3.417	33788
	200	3.059	84805	3.060	84806
	300	2.685	150342	2.686	150345

Table 1: Comparison of the values T_c and a_c calculated in present study (A) with those of Takhar et al. [17] (B) when N = 0, Q $\neq$ 0 for various values of μ (Conducting walls)

μ	Q	N	a_c	T_c
-1	0	0.0	3.998	18666
		0.5	3.566	13381
		1.0	3.004	9508
	10	0.0	4.167	24396
		0.5	3.503	16679
		1.0	2.662	10973
	50	0.0	4.480	50796
		0.5	2.349	28002
		1.0	2.034	14582
-0.75	0	0.0	3.406	10518
		0.5	3.232	7880
		1.0	3.107	6232
	10	0.0	3.661	15188
		0.5	3.334	10731
		1.0	3.108	8127
	50	0.0	4.037	36758
		0.5	3.066	21616
		1.0	2.585	14345
-0.50	0	0.0	3.197	6413
		0.5	3.128	5043
		1.0	3.079	4151
	10	0.0	3.427	9809
		0.5	3.245	7179
		1.0	3.129	5638
	50	0.0	3.720	26646
		0.5	3.047	15603
		1.0	2.766	10800

Table 2: The critical values of T_c and the corresponding values of a_c for assigned values of N, Q, μ (conducting walls)

μ	Q	N	a_c	T_c
-0.25	0	0.0	3.144	4461
		0.5	3.075	3491
		1.0	3.029	2866
	10	0.0	3.352	6954
		0.5	3.173	5029
		1.0	3.062	3925
	50	0.0	3.563	19930
		0.5	2.912	11131
		1.0	2.667	7576
0	0	0.0	3.126	3389
		0.5	3.036	2562
		1.0	2.976	2057
	10	0.0	3.326	5319
		0.5	3.107	3676
		1.0	2.980	2793
	50	0.0	3.497	15576
		0.5	2.761	7983
		1.0	2.525	5241
0.25	0	0.0	3.120	2724
		0.5	3.001	1962
		1.0	2.929	1530
	10	0.0	3.316	4287
		0.5	3.046	2785
		1.0	2.902	2047
	50	0.0	3.470	12664
		0.5	2.629	5830
		1.0	2.411	3682

Table 3: The critical values of T_c and the corresponding values of a_c for assigned values of N, Q, μ (conducting walls)

μ	Q	N	a_c	T_c
0.50	0	0.0	3.117	2275
		0.5	2.970	1552
		1.0	2.887	1175
	10	0.0	3.312	3582
		0.5	2.990	2173
		1.0	2.835	1545
	50	0.0	3.459	10622
		0.5	2.526	4363
		1.0	2.330	2664
0.75	0	0.0	3.116	1951
		0.5	2.942	1259
		1.0	2.850	926
	10	0.0	3.311	3074
		0.5	2.940	1739
		1.0	2.779	1198
	50	0.0	3.454	9126
		0.5	2.448	3351
		1.0	2.274	1991
1.0	0	0.0	3.116	1707
		0.5	2.917	1042
		1.0	2.819	746
	10	0.0	3.311	2690
		0.5	2.896	1420
		1.0	2.732	952
	50	0.0	3.454	7989
		0.5	2.389	2637
		1.0	2.235	1533

Table 4: The critical values of T_c and the corresponding values of a_c for assigned values of N, Q, μ (conducting walls)

μ	Q	N	a_c	T_c
-1.0	50	0.0	3.751	42781
		0.5	2.529	25080
		1.0	2.088	14378
	100	0.0	3.378	71516
		0.5	1.968	33644
		1.0	1.815	17784
	300	0.0	2.013	207803
		0.5	1.436	57124
		1.0	1.449	28191
-0.75	50	0.0	3.124	29825
		0.5	2.577	18168
		1.0	2.370	12618
	100	0.0	2.685	53007
		0.5	2.092	27339
		1.0	1.975	17665
	300	0.0	1.476	158027
		0.5	1.466	56713
		1.0	1.467	33035
-0.50	50	0.0	2.620	20506
		0.5	2.456	12778
		1.0	2.397	9262
	100	0.0	2.019	37894
		0.5	2.016	19998
		1.0	2.012	13564
	300	0.0	1.063	113060
		0.5	1.429	44370
		1.0	1.483	27280

Table 5: The critical values of T_c and the corresponding values of a_c for assigned values of N, Q, μ (non-conducting walls)

μ	Q	N	a_c	T_c
-0.25	50	0.0	2.429	14808
		0.5	2.342	8981
		1.0	2.312	6448
	100	0.0	1.788	27620
		0.5	1.903	14071
		1.0	1.937	9449
	300	0.0	0.957	82102
		0.5	1.360	31248
		1.0	1.433	19018
0	50	0.0	2.364	11392
		0.5	2.263	6433
		1.0	2.233	4482
	100	0.0	1.725	21298
		0.5	1.850	9901
		1.0	1.876	6450
	300	0.0	0.926	63208
		0.5	1.334	21354
		1.0	1.400	12637
0.25	50	0.0	2.340	9199
		0.5	2.212	4739
		1.0	2.180	3189
	100	0.0	1.700	17212
		0.5	1.822	7128
		1.0	1.844	4491
	300	0.0	0.914	51058
		0.5	1.335	14820
		1.0	1.392	8526

Table 6: The critical values of T_c and the corresponding values of a_c for assigned values of N, Q, μ (non-conducting walls)

μ	Q	N	a_c	T_c
0.5	50	0.0	2.332	7694
		0.5	2.179	3595
		1.0	2.145	2342
	100	0.0	1.692	14401
		0.5	1.810	5288
		1.0	1.828	3234
	300	0.0	0.911	42709
		0.5	1.346	10626
		1.0	1.395	5975
0.75	50	0.0	2.327	6604
		0.5	2.156	2802
		1.0	2.124	1774
	100	0.0	1.688	12361
		0.5	1.805	4042
		1.0	1.820	2412
	300	0.0	0.909	36658
		0.5	1.359	7889
		1.0	1.401	4358
1	50	0.0	2.327	5780
		0.5	2.139	2236
		1.0	2.108	1383
	100	0.0	1.687	10820
		0.5	1.804	3172
		1.0	1.816	1855
	300	0.0	0.908	32085
		0.5	1.371	6045
		1.0	1.407	3295

Table 7: The critical values of T_c and the corresponding values of a_c for assigned values of N, Q, μ (non-conducting walls)

Submitted on November 2005, revised on December 2005.

Stabilnost MHD Taylor-Couette-tečenja u uzanom procepu pri radijalnom zagrevanju i konstantnom toplotnom fluksu na spoljnom cilindru

UDK 537.84

Prikazana je linearna analiza stabilnosti hidrodinamičkog dispativnog Couette-tečenja viskoznog elektroprovodnog fluida izmedju obrtnih koncentričnih cilindara u prisustvu uniformnog uzdužnog magnetnog polja i konstantnog toplotnog fluksa na spoljnom cilindru. Jednačine za uzani procep u odnosu na osnosimetrične poremećaje su izvedene i rešene direktnim numeričkim postupkom. Posmatrana su oba tipa graničnih uslova sa provodnim i neprovodnim zidovima. Data je parametarska studija na osnovu μ, odnosa ugaone brzine spoljnog i unutrašnjeg cilindra, Q, Hartmann-ovog broja koji reprezentuje jačinu uzdužnog magnetnog polja, i N, odnosa Rayleigh-evog i Taylor-ovog broja koji prikazuje priraštaj toplote konstantnom brzinom ka spoljnom cilindru. Posmatrana su tri slučaja $\mu < 0$ (suprotno obrtanje), $\mu > 0$ (istosmerno obrtanje) i $\mu = 0$ (stacionarni spoljni cilindar) pri čemu je pretpostavljeno da je magnetski Prandtl-ov broj mali. Rezultati pokazuju da karakteristike stabilnosti uglavnom zavise od provodljivosti cilindara, a ne od toplotnog fluksa na spoljnom cilindru. Za razliku od prethodnih rezultata dobijenih za izotermsko i hidromagnetsko tečenje, kritični talasni broj je striktno opadajuća funkcija od Hartmann-ovog broja za provodljive zidove. Takodje, prisustvo konstantnog toplotnog fluksa dovodi do pada kritičnog talasnog broja za suprotno obrtne cilindre, što pokazuje da se za velike vrednosti -μ dešava prelaz od osnosimetričnog ka neosnosimetričnom poremećaju kako za hidrodinamičko tako i za hidromagnetsko tečenje i da se ovaj prelaz pojavljuje ranije ako magnetsko polje raste.